

DISCLAIMER

This report was prepared as an account of work sponsored by an agency of the United States Government. Neither the United States Government nor any agency thereof, nor any of their employees, makes any warranty, express or implied, or assumes any legal liability or responsibility for the accuracy, completeness, or usefulness of any information, apparatus, product, or process disclosed, or represents that its use would not infringe privately owned rights. Reference herein to any specific commercial product, process, or service by trade name, trademark, manufacturer, or otherwise does not necessarily constitute or imply its endorsement, recommendation, or favoring by the United States Government or any agency thereof. The views and opinions of authors expressed herein do not necessarily state or reflect those of the United States Government or any agency thereof.

THE OXIDATION BEHAVIOR OF TUNGSTEN
AND GERMANIUM ALLOYED MOLYBDENUM
DISILICIDE COATINGS

E. L. Courtright
R. A. Rapp

G. E. Wang
T. Kircher

November 1991

Presented at the
High Temperature Structural
Silicides Workshop
November 4-6, 1991
Gaithersburg, Maryland

Work supported by
the U.S. Department of Energy
under Contract DE-AC06-76RLO 1830

Pacific Northwest Laboratory
Richland, Washington 99352

MASTER



THE OXIDATION BEHAVIOR OF TUNGSTEN AND GERMANIUM ALLOYED MOLYBDENUM DISILICIDE COATINGS

Andrew Mueller*, Ge Wang, and Robert A. Rapp
Department of Materials Science and Engineering, The Ohio State University
Columbus, OH

Edward L. Courtright
Battelle Pacific Northwest Laboratory**
Richland, WA

T. Kircher
Aerospace Materials Division
Naval Air Development Center
Warminster, PA

* Present address: Armco Steel Co., Middletown, OH

** Operated for the U.S. Department of Energy by the Battelle Memorial
Institute

ABSTRACT

A multicomponent coating has been developed to protect Nb-base alloys from high-temperature oxidation. A solid solution of molybdenum and tungsten disilicide, (Mo,W)Si₂ provided the best results. This alloy composition was shown to support a slow-growing protective silica scale in service. Germanium additions made during the coating process helped to improve the cyclic oxidation resistance by increasing the thermal expansion coefficient of the silica scale. Germanium also helped to avoid "pestring" (accelerated low temperature oxidation) by providing better sealant coverage at low temperatures. The results of cyclic oxidation tests performed on coated Nb coupons at 900°C, 1370°C, and 1540°C in air are presented. The coated Nb successfully passed 200 one-hour cyclic oxidation tests at 1370°C and 60-h at 1540°C. Neither generalized accelerated low temperature oxidation or "pest" oxidation occurred when the coatings were exposed to isothermal conditions of up to 200-h in air in the temperature range 500-700°C.

INTRODUCTION

Niobium can be alloyed to improve its high temperature strength[1] and to some extent oxidation resistance.[2,3] If, compared to other structural alloys developed for oxidation resistance, niobium exhibits inherently poor high-temperature oxidation behavior because its oxide is not compact or impervious to permeation by molecular oxygen. The inward diffusion of oxygen anions results in a large molar volume increase at the metal/scale interface, which accumulates strain energy and leads to scale cracking. Since adequate resistance to high-temperature scaling cannot be achieved by alloying alone; a protective coating is necessary for any high-temperature application where niobium or niobium base alloys are expected to be used in oxidizing environments.

A multicomponent, redundant, protection approach must be employed if a long service life and cyclic oxidation resistance are both to be achieved. Essential components are: (a) a niobium-base alloy with good high-temperature creep strength and adequate inherent oxidation resistance to prevent catastrophic attack should the protective coating fail, (b) an effective bond layer/diffusion barrier to attach the protective coating and prevent inward diffusion of damaging interstitials (e.g. H, N, C, and O), (c) a compatible coating that serves as a reservoir for the protective component to support the growth of a compact oxide layer, and (d) a protective oxide layer that will continue to grow with time and prevent the ingress of oxygen.

BACKGROUND

Molybdenum disilicide (MoSi_2) was chosen as a reservoir from which a protective SiO_2 layer could be grown in service. The excellent high-temperature oxidation resistance of MoSi_2 has been previously established.[4,5,6] Coatings based on MoSi_2 have seen limited use, to date, because they are relatively brittle at room temperature and have low strength at high temperatures ($>1250^\circ\text{C}$).[7] In early studies involving impure material, "pest" oxidation, which is catastrophic oxidation at relatively low temperatures ($300\text{-}700^\circ\text{C}$), was observed.[8,9] The mismatch in thermal

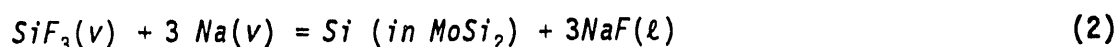
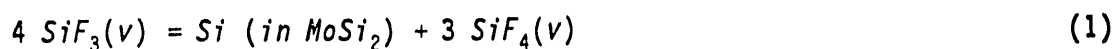
expansion coefficient between MoSi_2 and its thermally grown SiO_2 scale also led to spalling (i.e. decreased coating life) under thermal cycle conditions.

Potential solutions to these limitations are as follows: Tungsten (W) can be added to strengthen MoSi_2 at high temperatures.[10] This solid solution is currently used in high temperature furnace elements (Superkanthal™), which exhibit excellent oxidation resistance and sufficient high temperature strength. To increase the cyclic oxidation resistance and prevent peeling, germanium (Ge) additions have been effective.[6,11] Germanium forms a glass at lower temperatures than silicon, and therefore protects MoSi_2 in the lower temperature range where peeling is possible. The GeO_2 solute will decrease the SiO_2 glass viscosity at higher temperatures as well, but it also increases the coefficient of thermal expansion (CTE). The larger CTE minimizes the mismatch between the MoSi_2 coating and the protective silica layer.[12] Germanium additions to the SiO_2 film grown on MoSi_2 coatings have been shown to increase cyclic oxidation life by one order of magnitude.[13,14]

In this study, a two-step process was developed to produce $(\text{Mo,W})(\text{Si,Ge})_2$ diffusion coatings for the protection of Nb-base alloys.[15] In the first step, the deposition of a molybdenum layer (50-85 μm) or codeposition of molybdenum with 30 at% tungsten was performed by triode sputtering. The second step was the codeposition of silicon and germanium using a halide-activated pack cementation process to produce either $\text{Mo}(\text{Si,Ge})_2$ or a solid solution of $(\text{Mo,W})(\text{Si,Ge})_2$. Pack cementation is a self-contained chemical vapor deposition process in which the reactive vapor species are generated in situ. This process is carried out at high temperatures (900°C-1200°C) under an inert or reducing atmosphere to avoid oxidation of the substrate and the powdered masteralloy.

The substrate is embedded in a powder mixture or "pack", and sealed into an alumina crucible. A typical pack consists of three components: (1) a masteralloy or pure metal powder containing the element(s) to be incorporated into the substrate, (2) a halide activator salt (e.g. NaF, NaCl, etc.) and (3) an inert filler (e.g. Al_2O_3 , SiO_2 or SiC). The activator initially reacts

with the masteralloy, producing volatile metal halides. These volatile species diffuse to the substrate surface, driven by the chemical potential gradients of the elemental components between the pack and substrate, where a variety of reactions can contribute to the deposition of the coating element(s). The two most probable types of reactions are illustrated in Eqs. (1) and (2) for the siliconizing of molybdenum using a NaF activator.



Reaction (1) is a disproportionation-type reaction whereby a lower halide (SiF_3) reacts to form a higher halide to deposit silicon. In Eq. (2), a reaction occurs which deposits Si and a thin film of the liquid activator at the substrate surface. Because the volatile species in the Si-F system include major proportions of SiF_2 , SiF_3 , and SiF_4 , depending on the local activity for molecular fluorine, the deposition reaction can involve all of these volatile species.

EXPERIMENTAL APPROACH

Coating Development

A pure niobium rod was cut into disk coupons (16mm in diameter and 6mm in thickness) and these were sputter coated with pure Mo or a solid solution of Mo and W to a thickness of 50-85 μm . The measured and weighed coupons were embedded in a powder mixture containing between 7.5 and 17 wt.% pure Si powder (~325 mesh from AESAR), 3 wt% NaF (reagent grade from Alfa), and between 74.5 and 80 wt% SiC powder (120 grit from Metallurgical Supply Co.).

The substrate coupons and pack materials were placed into alumina crucibles and sealed with an alumina lid using an alumina-base cement. The sealed crucibles were then inserted into a combustion tube in an electric tube furnace, and pure Ar was introduced at a flow rate of approximately 100 ml/min. After the inert atmosphere had been established, the packs were

heated at 1150°C ($\pm 3^\circ\text{C}$) for various times. After diffusion, the packs were cooled back to room temperature in the Ar atmosphere. The coupons were then removed from the pack, and washed in hot water and ultrasonically cleaned in acetone to remove any salt condensate and loosely embedded pack material. Weight losses of the coupons after water-rinsing showed that some water-soluble substance, probably the NaF activator salt, was removed. Thickness and weight measurements were made on the cleaned coupons.

To codeposit two (Si plus Ge) or more elements by pack cementation, the partial pressures of gas species in the pack for the elements to be deposited must be comparable. If the gas specie(s) of one element is dominant, codeposition of the other specie(s) would be suppressed. The SOLGASMIX-PV calculation for the pack used in this study is reported elsewhere.[15] At 1400°K the partial pressure for SiF_3 and SiF_2 are 6.86×10^{-4} and 8.29×10^{-5} atm., and the partial pressure for GeF_2 is 2.04×10^{-5} atm. Since the gas diffusivity for all species is on the magnitude of $0.1 \text{ cm}^2/\text{s}$, the mass flux in the gas phase for a given drop in activity should be much greater than that in the solid phase where the diffusivity has a magnitude of about $10^{-10} \text{ cm}^2/\text{s}$. Therefore, the coating process should be nominally controlled by the solid-state diffusional growth of the silicide layer, which has been confirmed by kinetics analysis.[15] A Si-Ge alloy is also expected to form in the pack by the melting of Ge (melting point for Ge is 937°C). Thus, the activities of Si and Ge in the pack should each be less than unity, and will depend upon the original Si-to-Ge ratio in the pack.

Cyclic Oxidation Testing

Cyclic oxidation studies were conducted in air at 925°C , 1370°C , and 1540°C . The 925°C tests were performed at the NASA Lewis Research facilities.[16] The cyclic conditions consisted of a one hour soak period in air at temperature followed by a 20 minute cool down. The 1370°C tests were performed at the Ohio State University in an electric furnace with Superkanthal™ heating elements. The coupons were placed in a recrystallized high-purity alumina boat, and the boat was set on a high-alumina firebrick which was manually removed from the furnace during oxidation testing. The

thermal cycle program was one hour hot (at 1370°C) plus a half hour cool (setting outside the furnace). The weight-change of each coupon was measured by a Mettler™ AE163 digital balance.

Two coupons were tested at 1540°C at the Naval Air Development Center. These were performed using an automated balance and vertical tube furnace heated with Superkanthal™ elements. The specimens were contained within a high purity alumina crucible and suspended in the hot zone by an alumina rod. The heating cycle consisted of one hour at temperature in the hot zone and then the coupons were removed from the furnace and allowed to cool thirty minutes before reinserting. Weight gain was recorded at the end of pre-selected cycles.

Selected coupons were taken from the 1370°C oxidation test group and examined by X-ray diffraction in a Sintag diffractometer. Photomicrographs were also obtained from cross-sections prepared by standard metallographic procedures. A JOEL JXA-35 Scanning Electron Microscope (SEM) equipped with an Energy Dispersive Spectrometer (EDS) was used to examine the microstructures and compositions of the coatings. A CAMECA Electronprobe Microanalyser (EPMA) with Wave Dispersive Spectrometer (WDS) was also used to examine composition profiles. These analytical methods were especially useful for differentiating the silicon K-alpha radiation from tungsten M-alpha radiation, which are not distinguishable by EDS analysis.

RESULTS AND DISCUSSION

Coating Development

The coatings produced by pack cementation generally consisted of two layers: a thick outer MoSi_2 layer with a columnar morphology, and a very thin inner Mo_5Si_3 layer. Parabolic growth kinetics were observed for the MoSi_2 layers grown on pure Mo substrates at 1150°C. The rate constant was $9.31 \times 10^{-10} \text{ cm}^2/\text{s}$, and the activation energy for this process (900-1150°C) was calculated to be 58.3 kcal/mole, which is consistent with solid-state diffusion as the rate-

limiting step. This value agrees with the values (50-59 kcal/mole) reported for silicon diffusion in MoSi_2 . [17,18]

Germanium additions to MoSi_2 tended to retard coating growth. The morphologies of the duplex (Si,Ge) coatings were similar to those obtained for pure Mo, except that the thin Mo_5Si_3 intermediate layer formed on pure Mo was not present in the Mo-W disilicide. The germanium content was also lower at the external surface. An increase in the growth rate of the coating occurred when tungsten was added. Microhardness results showed that the room temperature hardness (and presumably the strength) also increased with increasing W content.

Cyclic Oxidation Testing

A summary of the cyclic oxidation results for coupons tested in air at 925°C is presented in Table I. Several samples failed prematurely due to oxidation in the holes that were drilled through the coupons for purposes of holding the button-shaped coupons during the sputtering process (this problem was corrected before further higher temperature testing continued). The coated areas looked very good with virtually no evidence of attack and one sample exceeded 200-h (cycles) of exposure. A photomicrograph of the coating at a corner section after 200-h is shown in Figure 1. A crack extends all the way to the niobium surface, but no serious oxidation has occurred indicating that the base of the crack is effectively sealed. The initial formation of Kirkendall porosity can be observed as a consequence of silicon redistribution. This porosity will grow with temperature and time as discussed in later sections.

Cyclic oxidation tests performed on coated Mo coupons and conducted in air at 1370°C showed that the germanium additions improved oxidation resistance. The Ge-doped coatings exhibited only a small weight gain, see Figure 2, and protected the Mo substrate, while the MoSi_2 coating without Ge suffered a significant weight loss, indicating a loss of volatile MoO_3 after a few cycles.

Cyclic oxidation tests were conducted on $\text{Mo}(\text{Si},\text{Ge})_2$ and $(\text{Mo},\text{W})(\text{Si},\text{Ge})_2$ coated niobium coupons for up to 200 one-hour cycles in air at 1370°C. Weight gains as a function of \sqrt{t} are presented in Figure 3. The kinetics indicate parabolic behavior following a transient oxidation period. The upper envelope curve (highest wt. gain) for $(\text{Mo},\text{W})(\text{Si},\text{Ge})_2$ coincides with the lowest envelope curve for $\text{Mo}(\text{Si},\text{Ge})_2$. From these results, it is clear that the Mo-30 at% W alloy coating has better oxidation resistance than the coating without tungsten. The lowest weight gain curves for the Mo,W alloy at 1370°C correspond to Bartlett's results[8] at 1330°C, but both are higher than the results Fitzer[11] reported at 1400°C.

A few of the coupons developed pin-holes at less than 50 cycles and a white oxide appeared on the surface. Analysis by X-ray and EDX showed this oxide to be Nb_2O_5 . The Nb_2O_5 reacted with the SiO_2 on the surface to form a white glassy film with continued testing. These samples were removed at this point and not subjected to extended testing, although they appeared capable of surviving many additional hours. The occurrence of the pinholes was found to coincide with the absence of an inner Mo_5Si_3 or Mo layer as seen in the Figure 1 micrograph and is primarily a coating layer uniformity problem. Two out of eight $\text{Mo}(\text{Si},\text{Ge})_2$ coated coupons (no tungsten) exceeded 200h; and six out of eight $(\text{Mo},\text{W})(\text{Si},\text{Ge})_2$ coated coupons (30 at.% tungsten) also passed 200-hour. The net weight gains for these coupons were in the range of 1.2-1.6 mg/cm^2 after a total of 200 one-hour cycles at 1370°C.

A corner section micrograph of a $\text{Mo}(\text{Si},\text{Ge})_2$ coating after twenty five hours at 1370°C is shown in Figure 4. The radial crack has been arrested by the inner silicide layer and deflected laterally. Cracks in the corner region are more severe due to the compliance required to accommodate the curvature. No oxidation has occurred in the niobium substrate due to the ability of the glass forming layer to effectively fill and seal the crack. A thick layer of protective $(\text{Si},\text{Ge})\text{O}_2$ on the surface provides evidence that this glass layer was able to resist spallation.

The weight gain kinetics for two $(\text{Mo},\text{W})(\text{Si},\text{Ge})_2$ coated coupons tested in air at 1540°C are shown in Figure 3, where a combination of transient and

parabolic oxidation behavior is again observed. These samples were terminated in good condition following 55-60-hours of cyclic exposure. The transient oxidation period is similar to 1370°C behavior, but the parabolic rate constant as defined by the linear portion of the curve of wt. gain vs \sqrt{t} [19] is higher, as expected.

A corner section micrograph of a niobium coupon coated with $(\text{Mo,W})(\text{Si,Ge})_2$ after 60-hour of cyclic oxidation in air at 1540°C is shown in Figure 5. The crack was deflected laterally in the underlying $(\text{Mo,W})_5(\text{Si,Ge})_3$ and sealed by the $(\text{Si,Ge})\text{O}_2$ glass. Porosity in the original $(\text{Mo,W})(\text{Si,Ge})_2$ has grown into a significant fraction of the coating volume compared to the lower temperatures, see Figures 1 and 4. While this porosity provides additional strain tolerance to thermal cycling, it also reflects a significant loss in the silicon reservoir needed to support continued SiO_2 growth.

Low Temperature Oxidation

Early reports of low temperature "pest" oxidation were attributed to the oxidation of microcracks[8] or diffusion of oxygen down grain boundaries.[9] However, recent work by Meschter[20] performed on high density, well characterized, good purity material did not observe "pestring" in either dry air, wet air, or oxygen between 400°C to 600°C.

New work by Meier, et al.[21] reports another type of generalized attack at low temperatures. Weight gains in excess of 5 mg/cm² after 80-hour of exposure in either air or oxygen were observed at 500°C. This phenomenon was attributed to the high volatility of MoO_3 at this temperature. The SiO_2 growth rate is too slow to be protective. Preoxidation at temperatures above 1000°C only delays the eventual onset of this generalized accelerated oxidation. At temperatures greater than 600°C, SiO_2 forms a protective film and suppresses MoO_3 vaporization. Oxidation then occurs at a very slow rate because the silica layer is continuous.

Three $(\text{Mo,W})(\text{Si,Ge})_2$ coated coupons were exposed to low temperature isothermal oxidation to determine if the coating was susceptible to either the

"pest" oxidation or generalized accelerated attack. After 192-hour of isothermal exposure at 500°C, 600°C, and 700°C in air, the recorded weight gains were 0.06, 0.16, and 0.10 mg/cm² respectively. The low weight gains and the good appearance of the test coupons suggest that the coating is not susceptible to either type of low temperature attack with the caveat that the data base is very limited.

X-Ray Diffraction Results

A partial X-ray diffraction pattern of the oxidized surface of a coupon coated with Mo(Si,Ge)₂ is shown in Figure 6. The third axis corresponds to the square-root of exposure time at 1370°C. Evidence of cristobalite forming at 1370°C under the cyclic exposure is seen although amorphous SiO₂ is still the dominate phase. The growth of the SiO₂ scale reduces the silicon content in the Mo(Si,Ge)₂ coating, and the lower silicide, Mo₅Si₃, forms underneath. After mechanical removal of the outer protective silicide layer, the x-ray pattern of the inner layer revealed the expected a Mo₅Si₃ structure. This layer exhibited a preferred orientation with very strong (002) and (004) peaks, indicating that the c-axis of the tetragonal structure is perpendicular to the surface of the coating.

SEM and EPMA Analysis

A cross-section of a coated Mo(Si,Ge)₂ coupon (no tungsten) oxidized at 1370°C for 10 one-hour cycles is shown in Figure 7a. Cracks that penetrated through the outer layer were stopped at the inner Mo₅Si₃ layer and sealed by the glass film. The EPMA compositional scan across this area (remote from cracks) is shown in Figure 7b. The coating is composed of two layers: an outer MoSi₂ layer containing some dissolved Ge and an inner Mo₅Si₃ layer with less germanium. A sharp drop in silicon content at the surface indicates a local depletion of silicon due to the formation of the silica scale.

The cross-section of a (Mo,W)(Si,Ge)₂ coated coupon (30 at% tungsten) oxidized in air at 1370°C for 26 one-hour cycles is shown in Figure 8a, and the associated EMPA compositional scan in Figure 8b. A two-layer morphology

was also developed, and again the cracks that penetrate the outer layer are also stopped by the inner layer. A larger number of voids were formed in the $(\text{Mo,W})(\text{Si,Ge})_2$ compared to the coatings with no tungsten. A schematic of these voids is illustrated in Figure 9. The voids form within a lighter appearing phase composed of $(\text{Mo,W})_5\text{Si}_3$, which is rich in tungsten. This optically light phase was found in the outer layers of tungsten-containing coatings and was continuous with the silicide in the inner layer. The tungsten rich composition is similar to that of the inner layer.

Silicon diffusion through the silicides requires a counterflow of vacancies in the silicon sublattice, or along phase interfaces. A large number of voids are thereby introduced into the lower silicide through vacancy condensation. The growth of the continuous phase inside the disilicide is aided by the short diffusion distance which results from the highly irregular morphology. A similar "interwoven" two-phase morphology has been observed for a certain type of solid-state displacement reaction, in which the forward motion of phase growth is repeatedly blocked by the accumulation of reaction products.[22,23] The irregular reaction interface can only occur in a system containing more than two components. In a binary system, a flat reaction interface is always required by the Phase Rule.

The voids formed within this coating should provide sites for stress relaxation (decreasing the effective Young's modulus of the coating layer) which may reduce the strain energy induced by thermal cycling and help interrupt crack propagation. In fact, the crack densities (number of cracks per unit length of surface) for the W-containing coupons were less than those for the coupons without tungsten by factor of 1.5. This observation suggests that tungsten additions provide both a reduced strain energy and a strengthening effect in the coating. In addition, the composite structure provides fast diffusion channels for transporting silicon to the coating/scale interface, where maintaining a sufficiently high Si activity is critical for exclusive growth of silica.

The microstructure of a $(\text{Mo,W})(\text{Si,Ge})_2$ coating (30 at% tungsten) after a total of 500-hour oxidation in air at 1370°C is shown in Figure 10(a). The

outer layer has become very porous compared to the inner layer, and is similar in appearance to Figure 4 which represents a shorter time at a higher temperature. A composition profile for this coating is shown in Figure 10(b). The outer layer is a two-phase structure, containing $(\text{Mo,W})(\text{Si,Ge})_2$ and a lower silicide $(\text{Mo,W})_5(\text{Si,Ge})_3$ which is the light phase. The inner layer is also a two-layered structure, with the outer portion consisting of a $60\mu\text{m}$ -thick $(\text{Mo,W,Nb})_5(\text{Si,Ge})_3$ and the inner portion is a $80\mu\text{m}$ thick and composed of $\text{Nb}_5(\text{Si,Ge})_3$. A significant amount of Ge (7at%) was found in the $\text{Nb}_5(\text{Si,Ge})_3$ compound. There is no distinct boundary between the two niobium containing silicides.

During oxidation, the silicon activity gradient in the as-grown disilicide is reversed, so that the thermodynamically stable Mo_5Si_3 is able to develop. Thus Mo_5Si_3 grew at the expense of both the outer disilicide and the original (Mo,W) layer. When the (Mo,W) layer is consumed, reaction between the lower silicide and the Nb substrate occurs. Niobium silicide Nb_5Si_3 was not prevalent at the lower-silicide/substrate interface for coupons exposed at 1370°C for short times; however, after extended exposure to high temperature (1370°C for 500h), the Nb_5Si_3 layer had developed. From the thicknesses of the Nb silicides and the exposure times, a parabolic rate constant for the growth of the Nb silicide at 1370°C was estimated at $2.0 \times 10^{-11} \text{cm}^2/\text{s}$. This value is an order of magnitude smaller than that for Mo_5Si_3 ($5 \times 10^{-10} \text{cm}^2/\text{s}$) at the same temperature.[17] A lower rate constant for Nb_5Si_3 growth means that this coating structure should have a longer diffusional service life than a MoSi_2 coating on pure Mo. A lower growth rate for a $(\text{Mo,Nb})_5\text{Si}_3$ layer than that for Mo_5Si_3 was also reported by Fitzer et al.[24]

CONCLUSIONS

A two-step coating process was used to produce a $(\text{Mo,W})(\text{Si,Ge})_2$ coating on niobium. After exposure to high temperatures, a lower silicide layer forms underneath and is effective in arresting cracks. The oxidation weight-gain kinetics are parabolic following an initial transient period. Test coupons

coated with $(\text{Mo,W})(\text{Si,Ge})_2$ passed 200 one-hour cycles at 1370°C and 60 one-hour cycles at 1540°C . These results, along with evidence of a thick protective glass layer, suggest that the germanium additions help cyclic oxidation resistance. The beneficial effects of the tungsten include the formation of microvoids, which provides a lower effective elastic modulus, and mechanical strengthening. No accelerated low temperature or "pest" oxidation was observed in the temperature range between $500\text{-}700^\circ\text{C}$. Thus, a $(\text{Mo,W})(\text{Si,Ge})$ multicomponent silicide coating offers significant promise for the protection of Nb-base alloys exposed to cyclic oxidizing environments over a broad range of temperatures.

ACKNOWLEDGEMENTS

This work was funded by NADC/DARPA project N62269/89/WX/00061. The authors thank Marshall Thomas for his encouragement and support. The authors appreciate the 925°C cyclic oxidation testing at NASA-Lewis Lab by Dr. James Smialek.

REFERENCES

1. R.T. Torgenson, *Columbium Metallurgy*, D.L. Douglass and F.W. Kunz (eds.), Interscience Publishers, NY, 1961.
2. H.P. Kling, *Technology of Columbium (Niobium)*, John Wiley and Sons, Inc., 1958.
3. F.J. Clauss and C.A. Barrett, *Technology of Columbium*, (ed.), John Wiley and Sons, Inc., 1958.
4. R.W. Bartlett, Air Force Material Laboratory, Technical Report ASD-TDR-63-753, Part III, September 1965.
5. J.B. Berkowitz-Mattuck and R.R. Dils, *J. Electrochem. Soc.*, 112 (1965), p. 583.
6. J. Schlichting, *High Temperature-High Pressures*, 10 (1978), p. 241.
7. P.J. Meschter and D.S. Schwartz, *JOM*, 11 (1989), p. 52.
8. J.B. Berkowitz-Mattuck, M. Rossetti and D.W. Lee, *Met. Trans.*, 1 (1970), p. 479.
9. J.H. Westbrook and D.L. Wood, *J. Nucl. Mater.*, 12 (1964), p. 208.
10. J.J. Petrovic, R.E. Hornell, "SiC Reinforced - MoSi₂/W Si₂ Alloy Matrix Composites", to be published.
11. E. Fitzner, *Ceramic Transactions, Vol. 10, Corrosive and Erosive Degradation of Ceramics*, R.B. Tressler and M. McNallon, (eds.), ACS, Westerville, OH, 1989, p. 19.
12. J. Schlichting and S. Neumann, *J. Non-Crystalline Solids*, 48 (1982), p. 185.
13. E. Fitzner and D. Kehr, *Thin Solid Films*, 39 (1976), p. 55.
14. E. Fitzner, H. Herbst and J. Schlichting, *Proceedings of the 4th International Conference on Carbon and Graphite*, (ed.), Session IX, London, 1974, p. 401.

15. A. Mueller, G.E. Wang, R.A. Rapp, and E.L. Courtright, "Development and Cyclic Oxidation Behavior of Protective (Mo,W)(Si,Ge)₂ Coatings on Nb-Base Alloys," submitted to *Journal of Electrochemical Society*.
16. Courtesy of J.L. Smialek.
17. R.W. Bartlett, P.R. Gage and P.A. Larssen, *Trans. AIME*, 230 (1964), p. 1528.
18. P. Kofstad, *High-Temperature Oxidation of Metals*, John Wiley and Sons, Inc., New York, 1966.
19. B. Pieraggi, *Oxidation of Metals*, 27(3,4), 1987, p. 177.
20. P.J. Meschter, "Low Temperature Oxidation of Molybdenum Disilicide," submitted to *Metallurgical Transactions*.
21. G.H. Meier, D. Berztiss, and F.S. Pettit, "Oxidation of MoSi₂ in the Temperature Range Between 500-1200°C, presented at Aero Mat '91, Long Beach, CA, 1991.
22. R.A. Rapp, A. Ezis, and G. Yurek, *Metall. Trans.*, 4 (1973), p. 1283.
23. C. Tanghitvittaya, J.P. Hirth, and R.A. Rapp, *Metall. Trans.*, 13A (1982), p. 585.
24. E. Fitzer, H. Herbst and J. Schlichting, *Werkstoffe und Korrosion*, 24 (1973), p. 274.

Table I. Summary of Cyclic Oxidation Results for
Niobium Coated (Mo,W)(Si,Ge)₂ Tested in Air at 925°C

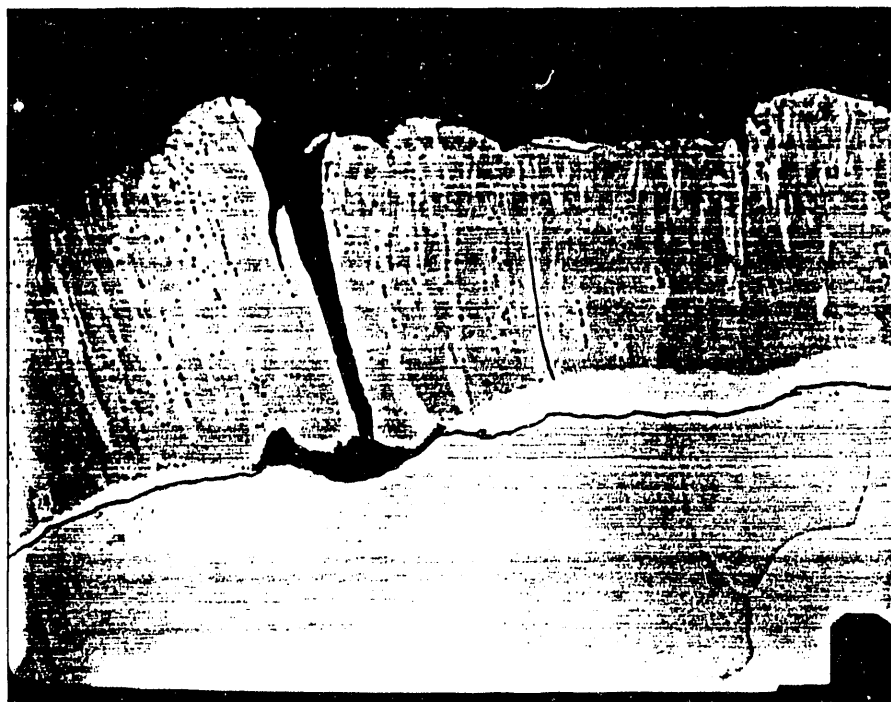
Internal Code	Substrate Material	Sputter Layer	Thickness (microns)	Pack Cementation	Minimum Cycle Life	Failure Mode
1	C-103	Mo *	67.31	Si	80	Hole Oxidation
2	Nb	Mo - 30 W	44.45	Si	>200	No Failure(+ 1.25 mg/cm ²)
3	Nb	Mo - 50 W	63.51	Si	200	Edge Oxidation + Nodules
4	Nb	Mo *	69.85	Low Ge	200	Hole Oxidation
5	C-103	Mo - 30 W *	74.93	Low Ge	60	Hole Oxidation + Nodules
6	WC3009	Mo - 30 W *	64.77	High Ge	40	Hole Oxidation

* Specimen contained holes used to hold the coupons for the sputter coating process.

Figure Captions

- Figure 1 Mo(Si,Ge)₂ coated niobium oxidized for 200 one-hour cycles at 925°C in air.
- Figure 2 Cyclic oxidation behavior of MoSi₂ coatings substrates with and without Ge additions on pure Mo at 1370°C in air.
- Figure 3 Oxidation kinetics for Mo(Si,Ge)₂ and (Mo,W)(Si,Ge)₂ coatings on niobium.
- Figure 4 Mo(Si,Ge)₂ coated niobium after 25 hours of cyclic oxidation testing in air at 1370°C.
- Figure 5 A (Mo,W)(Si,Ge)₂ coating after 60 hours of cyclic oxidation at 1540°C.
- Figure 6 X-ray diffraction pattern of an oxidized (Mo,W)(Si,Ge)₂ coupon, showing cristobalite formation during oxidation at 1370°C.
- Figure 7a Cross section of a Mo(Si,Ge)₂ coating after 10 one-hour cycles at 1370°C in air.

- Figure 7b EMPA composition profile of coating in Figure 7a.
- Figure 8a Cross section of a $(\text{Mo,W})(\text{Si,Ge})_2$ coating on niobium, after 26 one-hour cycles in air at 1370°C .
- Figure 8b EMPA composition profile of coating shown in Figure 8a.
- Figure 9 Schematic illustration showing void formation together with growth of the optically light $(\text{Mo,W})_5\text{Si}_3$ phase into the outer disilicide layer.
- Figure 10a Microstructure of a $(\text{Mo,W})(\text{Si,Ge})_2$ coating on niobium oxidation in air at 1370°C for a total 500-hours (including 144 one-hour cycles).
- Figure 10b EMPA compositional profile of coating shown in Figure 10a.



Mo(Si,Ge)₂

Mo

Nb

250x

40 μm

FIG 1

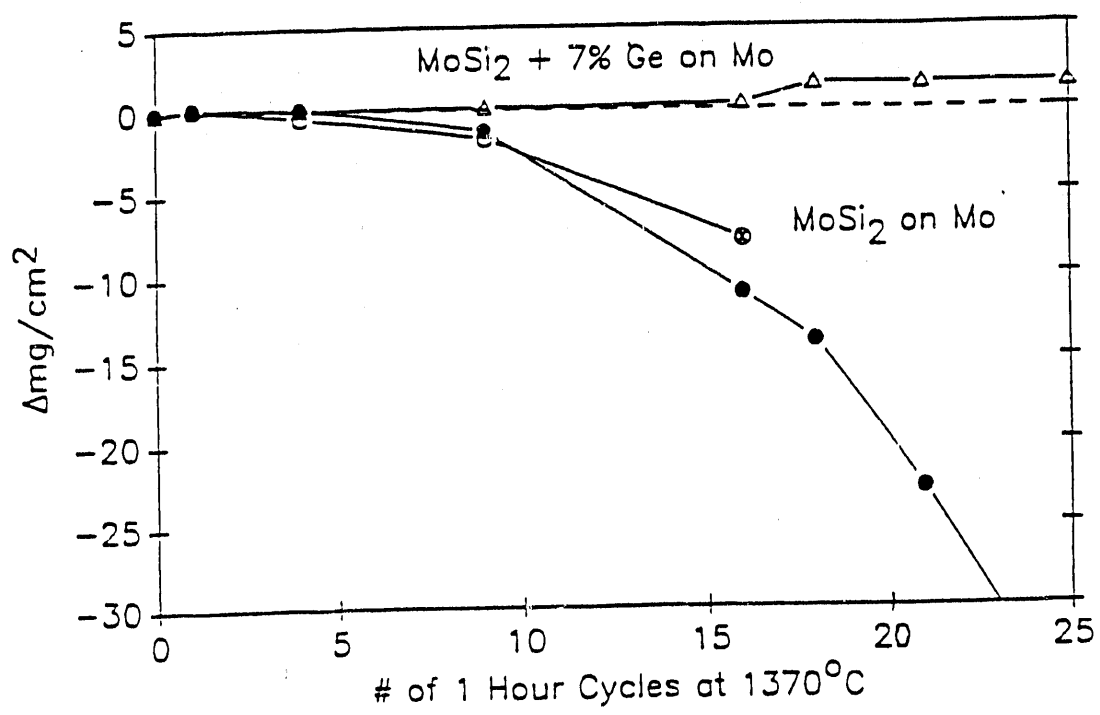


Fig 2

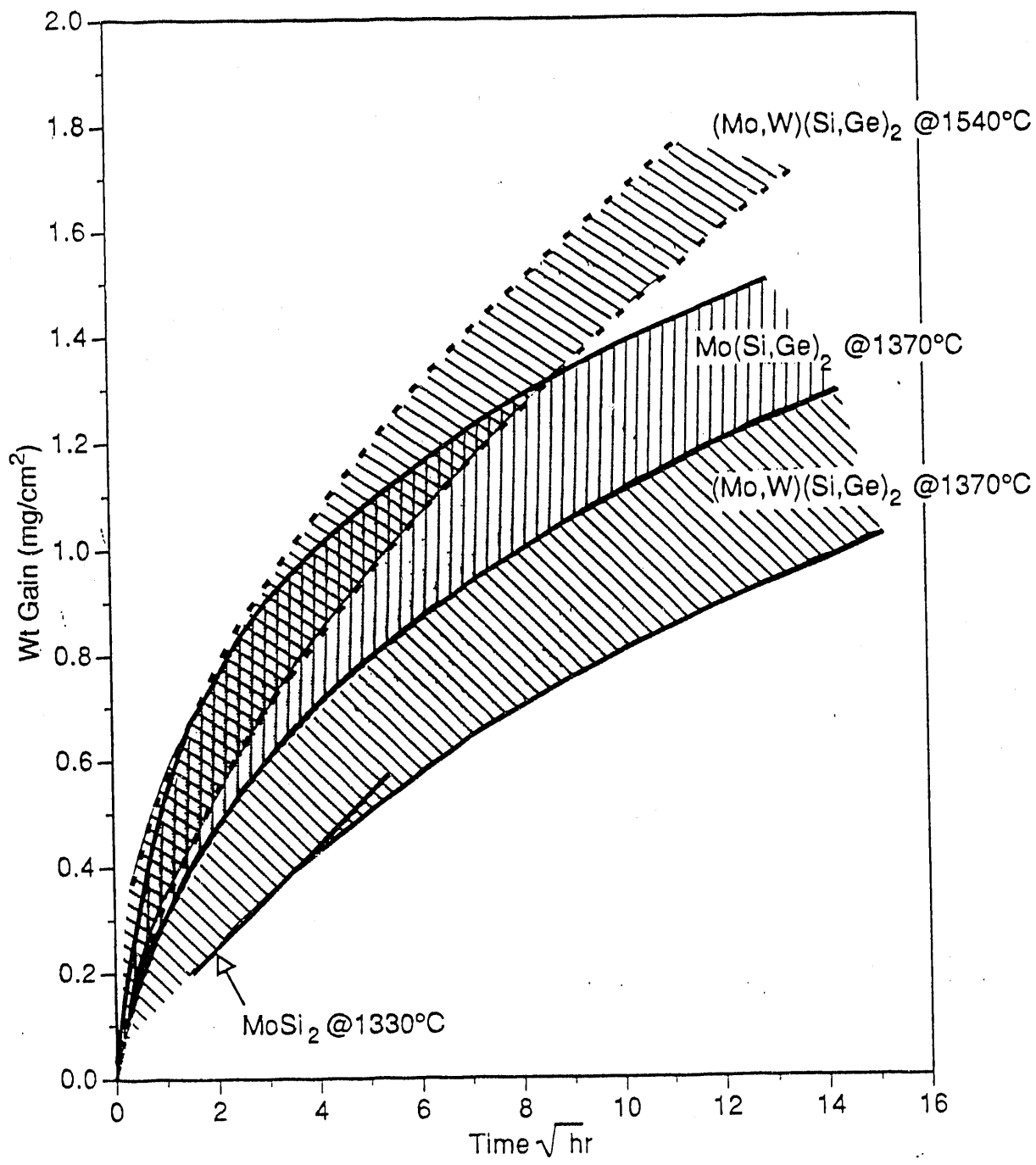
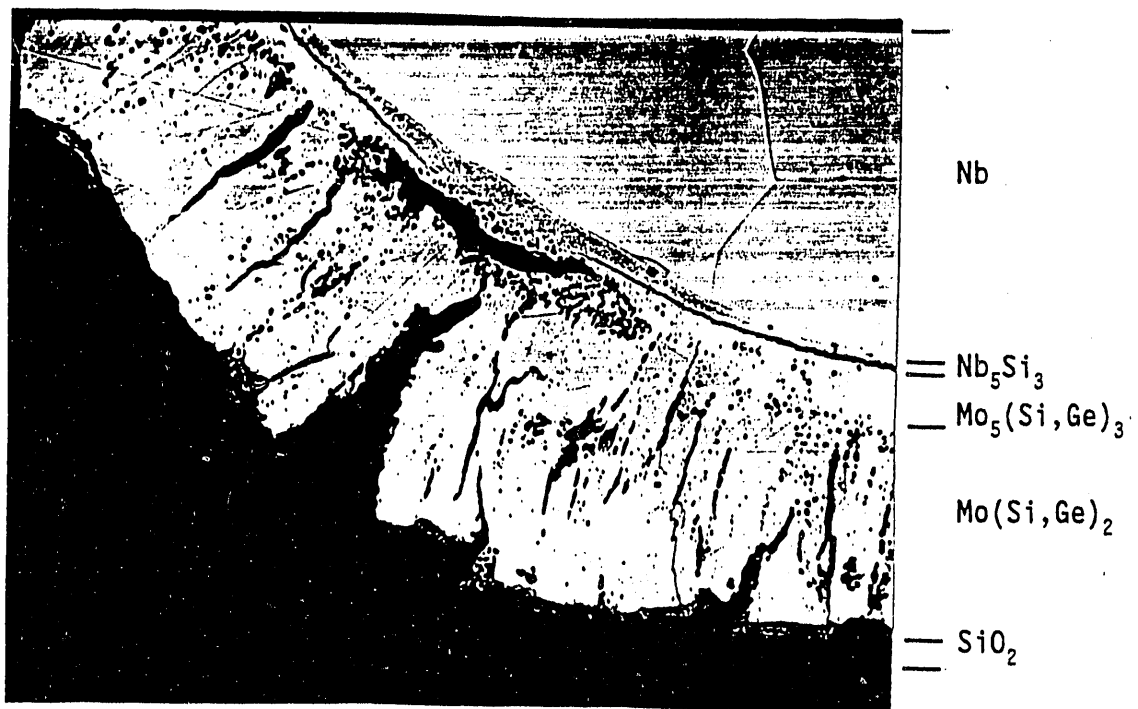


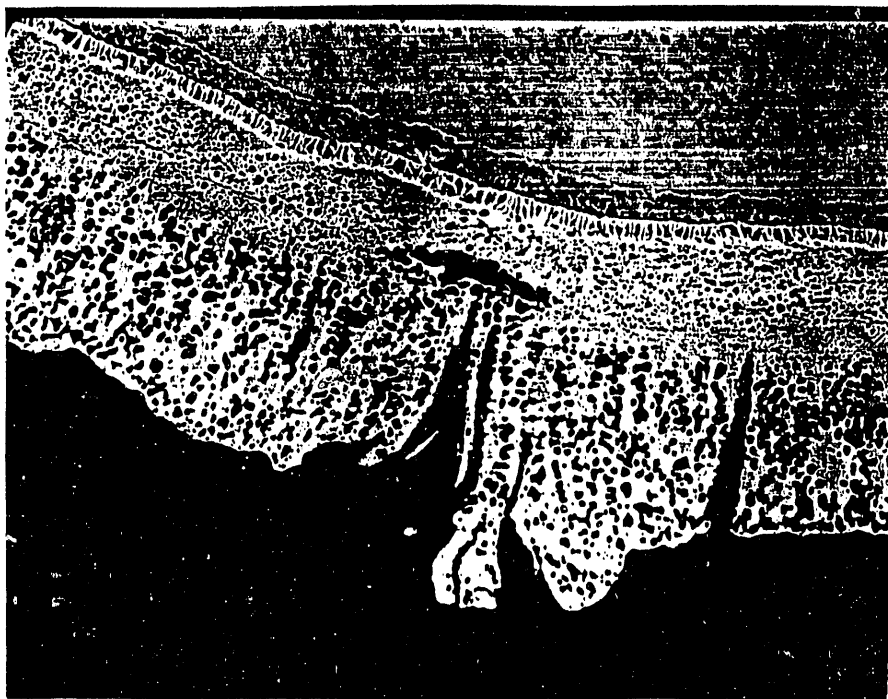
Fig 3



250x

40 μ m

FIG 4



- Nb
- $\text{Nb}_5(\text{Si}, \text{Ge})_3$
- $(\text{Mo}, \text{W}, \text{Nb})_5\text{Si}_3$
- $(\text{Mo}, \text{W})_5(\text{Si}, \text{Ge})_3$
- $(\text{Mo}, \text{W})_5(\text{Si}, \text{Ge})_3 + (\text{Mo}, \text{W})(\text{Si}, \text{Ge})_2$
- SiO_2

250x

40 μm

Fig 5

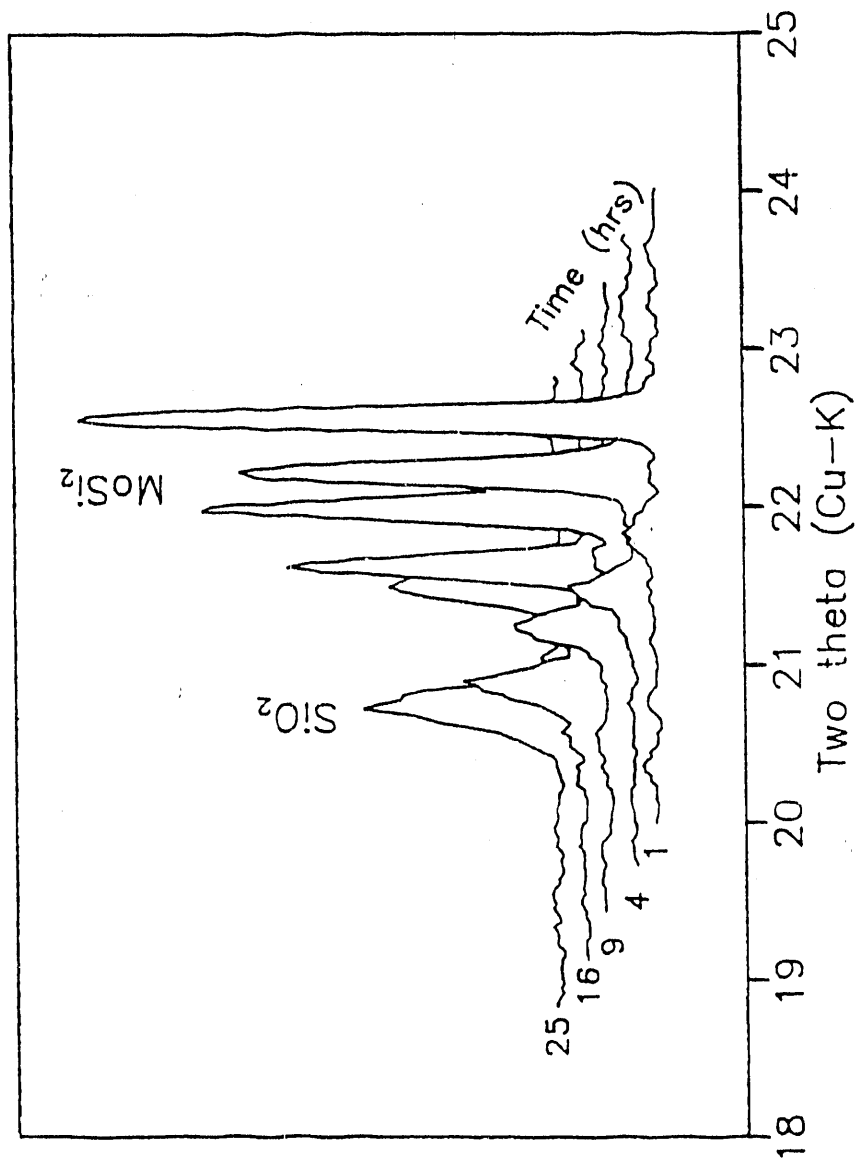
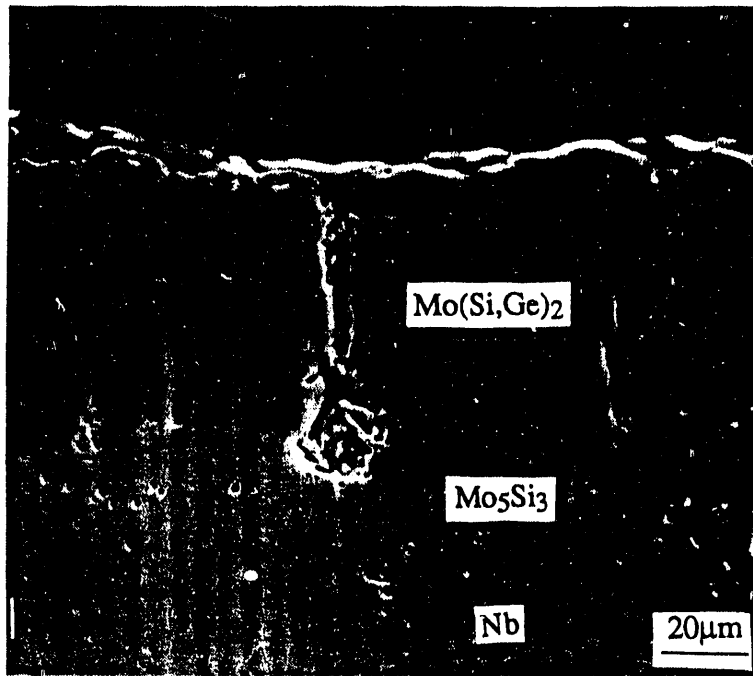
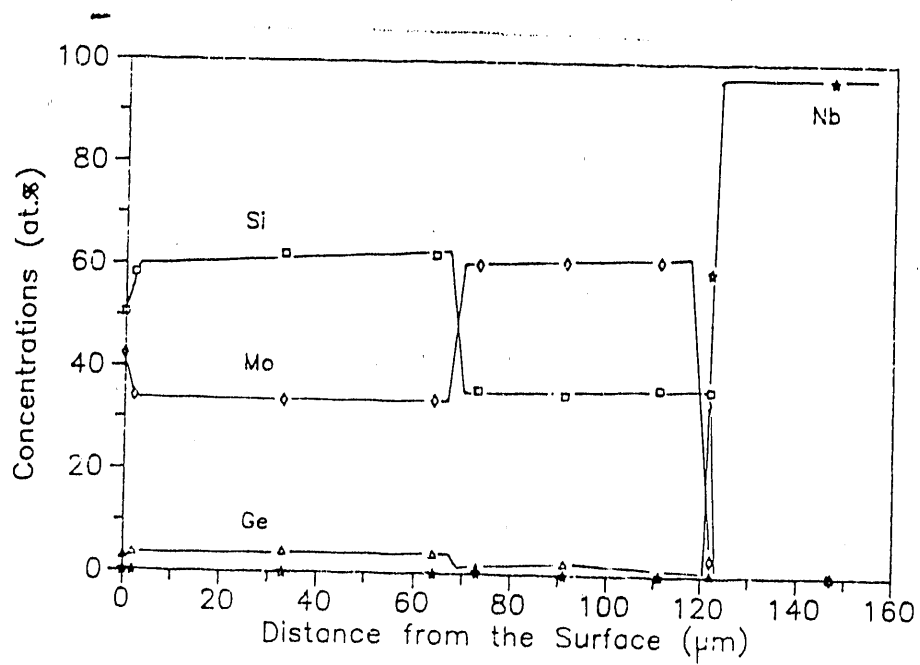


FIG 6

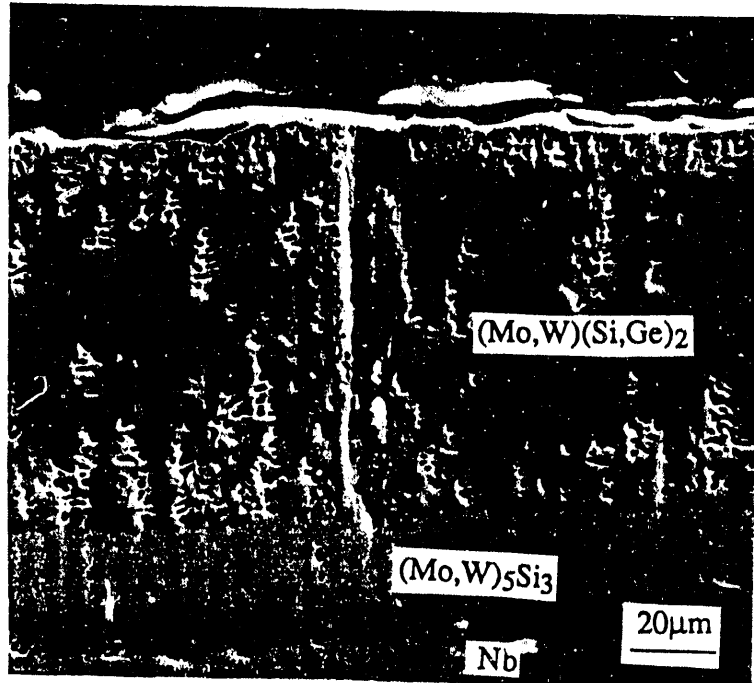


(a)

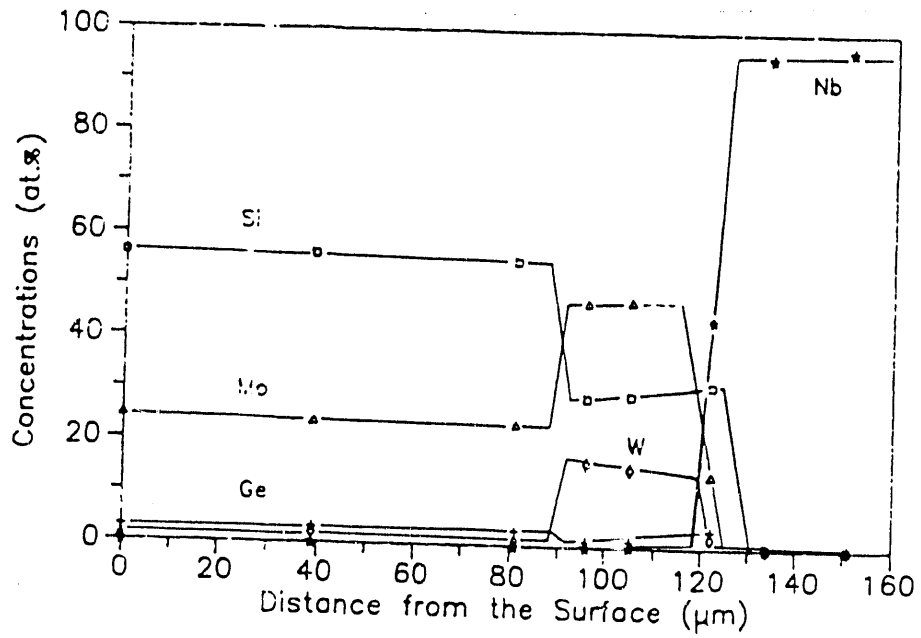


(b)

F.9 7



(a)



(b)

Fig. 8

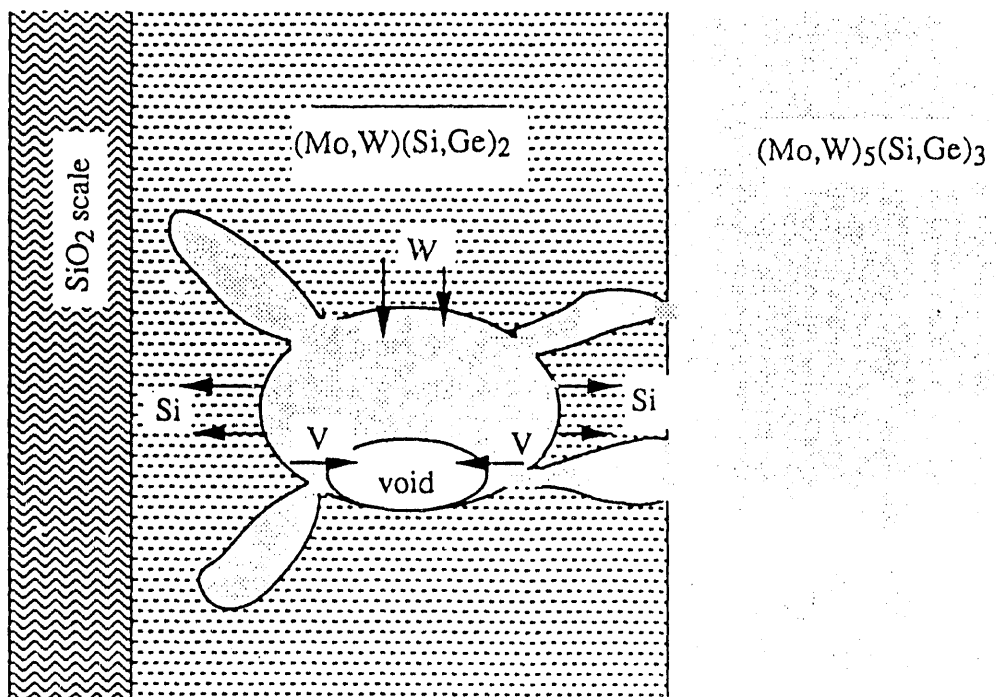
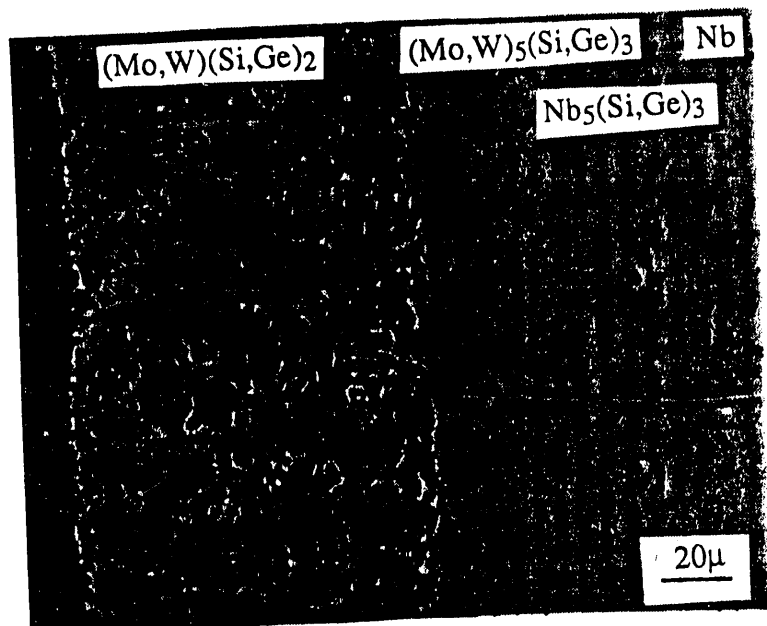
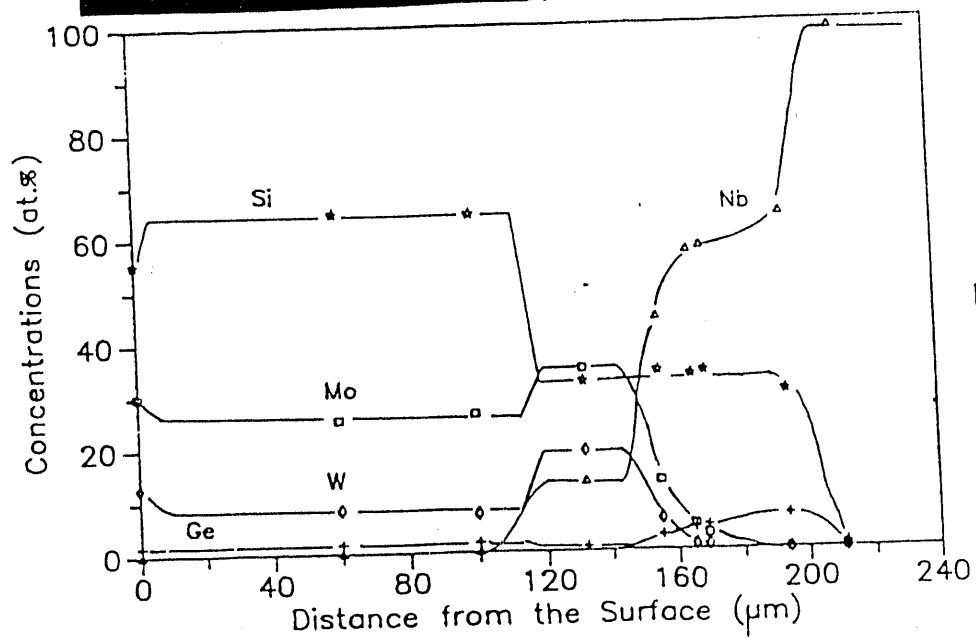


Fig 9



a)



b)

Fig 10

END

**DATE
FILMED**

3 / 17 / 92

